Energy Equity-constrained Tie-line Scheduling Model in Interconnected Systems

Sufan Jiang, *Member*, *IEEE*, Fangxing (Fran) Li, *Fellow*, *IEEE*, Xiaofei Wang, *Student Member*, *IEEE*, and Chenchen Li, *Student Member*, *IEEE*

***Abstract*—Energy equity refers to the condition in which access to the cleaner energy required by individuals is equally available to all. To relieve the energy expenditures – the key component in the concept of energy equity – of low-income communities, governments worldwide have imposed caps on soaring energy prices. However, the inherent mechanisms within the operational schedule remain undiscussed. This paper innovatively provides guidelines for operators to embed energy burden policies into the bulk power system model, by answering two critical questions. ① What is the impact on system price pattern when embedding the locational price constraints? ② How to reformulate the tie-line schedule to meet the equity thresholds? Consequently, a novel bi-level energy equity-constrained tie-line scheduling model is proposed. The conventional economic dispatch is solved at the upper level, and then a preliminary operational schedule is given to the lower level, where we propose an energy equity slackness component variable to evaluate the gap between preliminary and desired equity-satisfied operational schedules. The implicit constraints on the price are converted into explicit feasibility cuts with dual theory. Case studies on test systems demonstrate the reduced energy expenditure for underserved communities, and the optimal tie-line schedule is also validated.**

***Index Terms*—Energy equity, energy price cap, tie-line scheduling, feasibility cut, interconnected system.**

NOMENCLATURE

A. Sets

Ω_G	Set of generators
Ω_L	Set of transmission lines
Ω_w, Ω_D	Set of wind farms and loads
Φ, Θ	Feasibility sets for upper-level and lower-level models

B. Parameters

$\boldsymbol{a}, \boldsymbol{c}, \boldsymbol{B}, \boldsymbol{C}, \boldsymbol{G}, \boldsymbol{J}, \boldsymbol{H}, \boldsymbol{L}, \boldsymbol{K}, \boldsymbol{M}$	Coefficient matrices of proposed model
$\boldsymbol{b}, \boldsymbol{d}, \boldsymbol{g}, \boldsymbol{h}, \boldsymbol{f}$	Right-term parameters of proposed model
$c_{tie,t}$	Price of tie-line energy at time t
c_g	Generation cost of generator g
ec^{thd}	Imposed threshold of energy cost
F_l	Transmission limit of transmission lines
GSF	Generation shift factor
$P_{tie}^{\max}$, $P_{tie}^{\min}$	Upper and lower bounds of tie-line power flow
$P_g^{\max}$, $P_g^{\min}$	Upper and lower output limits of generator g
P_{dt}	Load of bus d at time t
u_{gt}	Status of generator g at time t
w_{mt}	Output of wind farm m at time t

C. Variables

$\rho_{gt}^{\max}$, $\rho_{gt}^{\min}$	Dual variables of unit output constraints
λ_t	Dual variable of system balance constraints
$\mu_{tl}^{\max}$, $\mu_{tl}^{\min}$	Dual variables of power flow constraints
$\boldsymbol{\delta}, \boldsymbol{\varepsilon}, \boldsymbol{\lambda}, \boldsymbol{\mu}, \boldsymbol{\rho}, \boldsymbol{\varphi}, \boldsymbol{\pi}, \boldsymbol{\sigma}, \boldsymbol{\zeta}$	Dual variables of proposed model in compact notation
$\boldsymbol{D}$	Load vector
es_{nt}	Energy equity slackness component variable for bus n at time t
L	Lagrangian function of economic dispatch (ED) problem
M_{big}	Sufficient big constant
$P_{tie,t}$	Energy flow on tie-line at time t
P_{gt}	Power output of generator g at time t
$\boldsymbol{P}, \boldsymbol{y}$	Variables of proposed model in compact notation
$\boldsymbol{s}$	Vector of energy equity slackness variable
$z_{gt}^{\mu,\max}$, $z_{gt}^{\mu,\min}$, $z_{gt}^{\rho,\max}$, $z_{gt}^{\rho,\min}$	Binary auxiliary variables under Karush-Kuhn-Tucker (KKT) conditions
$\bar{\boldsymbol{z}}_{\boldsymbol{\rho}}$, $\bar{\boldsymbol{z}}_{\boldsymbol{\mu}}$	Results of $\boldsymbol{z}_{\boldsymbol{\rho}}$ and $\boldsymbol{z}_{\boldsymbol{\mu}}$ from upper level
$\boldsymbol{z}_{\boldsymbol{\rho}}$, $\boldsymbol{z}_{\boldsymbol{\mu}}$	Auxiliary binary variable vectors

I. INTRODUCTION

DURING the transition to lower-carbon energy sources, it is required that the benefits in the energy system through the intentional design of systems, technologies, procedures, and policies are distributed in fairness and justice [1]. Therefore, the evolving social and policy climate has placed new explicit requirements to integrate energy equity and justice strategies [2]. In the U.S., families with annual

Manuscript received: May 21, 2024; revised: July 9, 2024; accepted: August 28, 2024. Date of CrossCheck: August 28, 2024. Date of online publication: November 19, 2024.

S. Jiang, F. Li (corresponding author), X. Wang, and C. Li are with the Department of Electrical Engineering and Computer Science, University of Tennessee, Knoxville, TN 37996, USA (e-mail: sjiang22@utk.edu; fli6@utk.edu; xiaofeiwang96@gmail.com; cli66@utk.edu).

DOI: 10.35833/MPCE.2024.000529

incomes below \$52492 for two adults and two related children in 2020 are often classified as "low-income" [3], and 60% of these low-income families (i.e., 15.4 million households) spend more than 10% of the household's income on energy bills [4]. Communities that often experience racial segregation, high unemployment rate, poor housing conditions, and barriers to accessing financing and investment are more likely to suffer from energy inequity issues [5].

Public participation and intervenor compensation are critical energy equity tools. Appropriate metrics are also needed to track and evaluate the results of policies, regulations, and programs intended to deliver equitable outcomes [6]. As needed for successful energy equity initiatives, countries around the world have developed varying strategies supporting the energy needs of low-income households [7]. In the U.S., the Weatherization Assistance Program (WAP) [8] aims to increase the energy efficiency of dwellings, and the Low-income Home Energy Assistance Program (LIHEAP) provides assistance with home energy bills [9], which has established a formula for distributing funds for both weatherization assistance and helping low-income households meet their immediate home energy needs. Since 2022, the French government has taken steps to keep energy costs down by limiting the increase of electricity prices within 4% [10]; the state-owned energy giant Electricité de France (EDF) will take an €8.4 billion (£7 billion) financial hit as a result of this decision. In Denmark, around 0.44 million low-income families were entitled to a tax-free cheque from the government to help them cover their costs in 2022 [11]. In the UK, the government has imposed a price cap on standard variable tariffs and default tariffs based on the estimated costs of supplying electricity and gas [12].

The above governmental programs made remarkable efforts in providing affordable and accessible cleaner energy equitably. While few of them have created an environment for the operators to consider the energy equity issues within the utility models [13], this is mainly because the traditional market structure may not have economic incentives to make equity-based investments. Therefore, it is critical for state regulators and utilities to establish the policy ecosystem to implement low-income energy programs [14]. The ultimate goal is to convert the energy equity policies into technical constraints that can be implemented in the utility model. To some extent, the interventions on the traditional locational marginal prices (LMPs) are inevitable due to the enforced equity constraints. Our previous work [15] has made some explorations on novel planning models from a utility perspective to embed the energy equity constraints. Note that the energy equity considerations in utility regulation are advocated by various sectors in societies rather than purely driven by economics [6]; in other words, the interventions on the dispatch models act as policy constraints, and the resultant nodal price will not only signal the transmission constraints but the energy equity policy constraints as well. Furthermore, it is needed to evaluate indicators [16] for policies, regulations, and programs to bring the overall best outcomes on both cost and equity. For example, in [17], the total health benefits are adopted to evaluate the economic value of conventional plant replacement by energy storage. In 2021, the Oregon legislative session passed law HB 3141 to increase the funding for low-income weatherization and direct the setting of equity metrics for all funds invested by the Energy Trust of Oregon [18]. The intervenor funding for an equity program, such as the LIHEAP program introduced in [9], needs to be sufficient and reliable to provide meaningful cost reduction for low-income households. Compared with the conventional utility model, the additional costs in the widely advocated equity programs are denoted as "social cost" in this paper, the sustainability of which is crucial because the energy equity issues are chronic for the holistic system [19].

For the aforementioned programs, the internal mechanisms of corresponding market models are significant to developing energy equity-based technologies, procedures, and policies. Although the implications of traditional market models are modified by the novel mechanisms, we regard this as a "market mechanism extension" rather than "market distortion". The developed model remains optimal within the proposed environment for novel market mechanisms. Entities conventionally participate in day-ahead [20], [21] and real-time markets [22], [23]. Within more flexible and reliable electricity markets [24], [25], novel pricing methods [26], [27] are developed as supplementation to the LMPs to accommodate the advanced demand response and environmental-friendly policy. In terms of price intervention studies, it is recommended in [28] that, compared with revenue caps, the price cap regulation is more desirable, especially in developing economies that often experience substantial inflationary pressures. The price cap is claimed as one of the regulatory tools [29], as policymakers have always created incentives for adequate investment in electricity generation, yet low, non-volatile prices are also required. Reference [30] compares two alternative mechanisms for capping prices in two-settlement electricity markets. The regulatory intervention to the spot prices is one of the approaches; it is concluded that a forward cap increases the firms' incentives for forward contracting, whereas a spot cap reduces such incentives. The theory and practice of price cap regulation for utilities are assessed in [31], and the regulatory commitment is significant in promoting long-term investment incentives. A pure price cap is optimal when the interests of both producer and consumer are equally weighted, while the promotions for the spot investments remain concerns. Note that in the above research work, incentive mechanisms and market models are developed under economic orientation, which means that the recently advocated energy equity concerns are still expected in a novel utility model from the policy perspective. This is also one of the critical motivations and research gaps in this paper.

Further, in interconnected systems, the tie-line schedule significantly impacts the prices of each system, and consequently, impacts the consumer payment and energy burden of each community in the entire interconnected system. Therefore, interchange trading in interconnected systems [32], [33] is also focused on in this paper. Works have been made to solve the joint dispatch problem in a distributed fashion, focusing on primal [34] and dual decomposition methods [35]. To account for the cost of losses and avoid tie-line flow with zero price difference, the loss factors are introduced in [36] when clearing the nodal and zonal pricing markets. Interchange flow is also cleared in ancillary service markets [37], wherein new incentive mechanisms [38] are proposed to elicit truthful bids from profit-maximizing units. In interconnected systems, each independent system operator (ISO) does not have access to the full operational information [39] of another balancing area (BA), thus distributed algorithms are adopted to solve the global problem in decentralized manners [40], [41].

According to the aforementioned introduction, the operators from the areas with energy equity issues (e.g., higher energy burdens) are expecting the designs and implementations of specific equity-concerned policies. However, in multi-area systems, the price information is determined by operational details which are preserved by local ISOs [42]. As a result, the critical research gaps lie in how to build novel trading models for tie-line schedules in interconnected systems, to achieve the desired price pattern when accommodating the energy equity requirements. Note that the system operators ensure grid reliability and stability, and market operators embed these requirements as constraints. Therefore, in this paper, the market operators conduct most of the activities.

To fill the research gaps discussed above, a novel tie-line scheduling model is proposed that provides guidelines to market operators for the scheduling strategy and subsidy policy needed when enforcing the energy equity policies. At the upper level of the proposed model, the conventional economic dispatch (ED) problem is solved, and then the preliminary operational schedule is given to the lower-level model. At the lower level, an energy equity slackness component (EESC) variable is proposed, which can evaluate the typical characteristics of the gap between the given operational schedule and the desired schedule that meets the energy equity constraints. Subsequently, the duality theorem is adopted to solve the lower-level model, wherein the implicit social-driven locational price constraints are converted into explicit feasibility cuts, which are sent back to the upper level to iteratively prune the infeasible region of the model. To further integrate the features of the subsidy policy into the energy equity-constrained market, the feasibility cuts are modified as improved optimality cuts, and thereby the model convergence is accelerated. The proposed bi-level tie-line scheduling model provides guidelines to the market operators for how to reformulate operational schedules to achieve the desired system energy price pattern, as well as how to achieve the expected subsidy policy when operational flexibilities are exhausted.

The main contributions of this paper are summarized as follows.

1) A novel bi-level energy equity-constrained tie-line scheduling model for interconnected systems is proposed to embed the energy burden constraints. The model innovatively reveals the inherent mechanism for reformulating tie-line schedules to achieve the desired energy price pattern following the requirements of energy equity policies.

2) In the proposed model, an EESC variable is proposed to relax the lower-level model and also to evaluate the typical characteristics of the gap between the preliminary and the desired energy equity-satisfied operational schedules.

3) The duality theorem is adopted to convert the implicit social-driven cost constraints into explicit feasibility cuts, which are further modified as improved optimality cuts when considering the features of subsidy policy, and consequently accelerate the convergence of the model.

The rest of this paper is organized as follows. Section II presents the energy equity-constrained ED problem, and validates the implicit traits of the energy equity constraints. Section III introduces the proposed bi-level energy equity-constrained tie-line scheduling model. Section IV discusses the solution methodology. Section V gives the computational results. And Section VI presents the concluding remarks.

II. Energy Equity-constrained ED Problem

In this paper, we aim to implement the energy expenditure threshold for low-income communities, acting as price cap constraints into the conventional ED problem. The diagram of a two-area interconnected system is adopted. As shown in Fig. 1, area A (sending-end) and area B (receiving-end) are operated independently. It is assumed that the energy inequity problems occur in the receiving-end (denoted as R-end hereafter), as a result, in this paper, we mainly focus on the methods that embed the energy expenditure constraints into the ED problem of R-end.

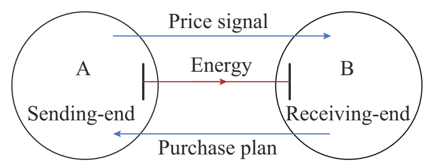

Fig. 1. Diagram of a two-area interconnected system.

In the two-area interconnected system, the sending-end (denoted as S-end hereafter) sends the tie-line price signal to the R-end, and the R-end puts the price into the ED problem, and then returns the purchase plan to the S-end. The ED problem of R-end with energy expenditure constraints (price caps) is presented as follows.

$$\min\left(\sum_t c_{tie,t}P_{tie,t} + \sum_t\sum_{g\in\Omega_G} c_g P_{gt}\right) \tag{1}$$

s.t.

$$u_{gt}P_g^{\min} \le P_{g,t} \le u_{gt}P_g^{\max} \quad \forall g, \forall t \tag{2}$$

$$P_{tie}^{\min} \le P_{tie,t} \le P_{tie}^{\max} \quad \forall t \tag{3}$$

$$P_{tie,t} + \sum_{m\in\Omega_w} w_{mt} + \sum_{g\in\Omega_G} P_{gt} = \sum_{d\in\Omega_D} P_{dt} \quad \forall t \tag{4}$$

$$\begin{aligned} -F_l \le GSF_{tie-l}\cdot P_{tie,t} + \sum_{g\in\Omega_G} GSF_{g-l}\cdot P_{gt} + \sum_{m\in\Omega_w} GSF_{m-l}\cdot w_{mt} - \\ \sum_{d\in\Omega_D} GSF_{d-l}\cdot P_{dt} \le F_l \quad \forall t, \forall l\in\Omega_L \end{aligned} \tag{5}$$

$$\sum_t\left[-\lambda_t + GSF_{n^{eb}-l}\cdot\left(\mu_{tl}^{\min}-\mu_{tl}^{\max}\right)\right]P_{d(n^{eb})t} \le ec^{thd} \tag{6}$$

In the objective function (1), the first term is the tie-line energy importing cost, and the second term is the generation cost. Constraint (2) gives the upper and lower output limits of generators. In this paper, we assume that the commitment decision of the generators is given priority, then the status u_{gt} denotes the parameters in this model. But note that the proposed model is scalable to solve the unit commitment (UC) problem. Constraint (3) gives the transmission limits of the tie-line. In the proposed model, we assume that there is only one tie-line connecting the two areas, but it is easy to expand to multiple tie-lines. Equation (4) gives the system energy balance constraints. For clarity, the uncertainty of renewable energy sources (represented by w_{mt} in this paper) is not considered, but we plan to study this in subsequent works using robust or stochastic methods. Constraint (5) gives the DC power flow model, wherein GSF describes the sensitivities of line flow with respect to node injection, e.g., GSF_{g-l} is the sensitivity of line l with respect to the power injection of generator g; and n^{eb} is the index of node with energy burden. And constraint (6) is the energy expenditure threshold, of which the first term is the expression of the LMP, the second term $P_{d(n^{eb})t}$ is the load of the low-income bus, and the given energy cost threshold is denoted as ec^{thd}. Note that in (6), the LMP expression comes from the Lagrangian multipliers λ and μ, which are the dual variables of the original ED problem (1)-(5). According to the duality theorem, the dual variables are unique if the original ED problem (1)-(5) is determined. Consequently, the feasibility of the energy expenditure-constrained ED problem (1)-(6) can not be ensured. In this case, we propose a novel bi-level energy equity-constrained tie-line scheduling model, aiming to adjust the imported price c_{tie} by strategically making tie-line purchase plan P_{tie}.

III. Bi-level Energy Equity-constrained Tie-line Scheduling Model

According to the illustration in Section II, the LMPs are determined by the conventional ED problem. Therefore, the requirements for P_{tie} should be explored to ensure the model feasibility after embedding the energy cost threshold constraints.

A. Description of Proposed Model

A novel bi-level energy equity-constrained tie-line scheduling model is proposed in this subsection. The desired price pattern is approached by iteratively reformulating the tie-line schedule in a bi-level structure, i.e., the novel ED problem enforces the social-driven energy cost constraints in a hierarchical way. The model is reformulated in (1)-(6), with the objective in (1) and constraints in (2)-(5) and (7)-(16).

$$P_{tie,t} \in \Phi \tag{7}$$

$$\Phi := \left\{ P_{tie,t} \middle| \min_{P_g, es, \lambda, \mu, \rho, z^{\rho}, z^{\mu}} \sum_t es_{n^{eb}t} = 0 \right\} \tag{8}$$

$$\sum_t \left[-\lambda_t + GSF_{n^{eb}-l} \cdot \left(\mu_{tl}^{\min} - \mu_{tl}^{\max} \right) - es_{n^{eb}t} \right] P_{d(n^{eb})t} \le ec^{thd} \tag{9}$$

$$0 \le es_{n^{eb}t} \le -\lambda_t + GSF_{n^{eb}-l} \cdot \left(\mu_{tl}^{\min} - \mu_{tl}^{\max} \right) \tag{10}$$

$$\lambda, \mu \in \Theta \tag{11}$$

$$\Theta := \left\{ (2), (4), (5), (13)\text{-}(16) \right\} \tag{12}$$

$$\begin{cases} \rho_{gt}^{\max} \le M_{big} z_{gt}^{\rho,\max} \\ M_{big}\left(z_{gt}^{\rho,\max} - 1 \right) \le P_{gt} - u_{gt} P_g^{\max} \end{cases} \tag{13}$$

$$\begin{cases} \rho_{gt}^{\min} \le M_{big} z_{gt}^{\rho,\min} \\ M_{big}\left(z_{gt}^{\rho,\min} - 1 \right) \le u_{gt} P_g^{\min} - P_{g,t} \end{cases} \tag{14}$$

$$\begin{cases} \mu_{tl}^{\max} \le M_{big} z_{gt}^{\mu,\max} \\ M_{big}\left(z_{gt}^{\mu,\max} - 1 \right) \le GSF_{tie-l} \cdot P_{tie,t} + \sum_{g \in \Omega_G} GSF_{g-l} \cdot P_{gt} + \\ \qquad \sum_{m \in \Omega_w} GSF_{m-l} \cdot w_{mt} - \sum_{d \in \Omega_D} GSF_{d-l} \cdot P_{dt} - F_l \end{cases} \tag{15}$$

$$\frac{\partial L}{\partial P_g} = \sum_t \sum_{g \in \Omega_G} c_{gt} + \sum_t \sum_{g \in \Omega_G} \left(\rho_{gt}^{\max} - \rho_{gt}^{\min} \right) + \sum_t \lambda_t + \sum_t \sum_{l \in \Omega_L} \left(\mu_{tl}^{\max} - \mu_{tl}^{\min} \right) \cdot GSF_{g-l} = 0 \tag{16}$$

Based on the preceding discussion, the market operator at the R-end strategically submits the purchase plan of tie-line energy to the S-end, to regulate the local price pattern. Therefore, in (7), the tie-line energy $P_{tie,t}$ should belong to a feasibility set Φ, which is depicted by (8)-(16). This set itself, also has objective function and constraints that are modeled with given $P_{tie,t}$. In (9), we propose an EESC variable es_{nt} to evaluate the gap between the existing operational schedule and the target operational schedule, which is subject to the mandatory energy cost threshold ec^{thd}. Ultimately, this gap between the existing and desired schedules, e.g., the slack variable es_{nt}, should be tuned down to 0, as illustrated by objective function (8), if the energy cost threshold is violated initially. The EESC variable is bounded by (10), indicating that the slack variables should not exceed the nodal LMP. Note that the LMPs are expressed by dual variables λ and μ, and therefore, the dual variables also belong to a feasibility set Θ, which denotes the complete Karush-Kuhn-Tucker (KKT) conditions of the model (1)-(5). Equation (12) gives the primal feasibility conditions; (13)-(15) are the linearized complementarity slackness conditions using big-M methods, where ρ, λ, and μ are the dual variables of constraints (2), (4), and (5), respectively; and (16) is the stationarity constraint.

In conclusion, the proposed model consists of two layers. At the upper level, the model (1)-(5) solves the classical ED problem; and at the lower level, the model (7)-(15) first proposes an EESC variable to create a relaxed structure, and consequently, the typical characteristics of the gap between the existing operational schedule to the energy equity-constrained operational schedule are evaluated. Based on this bi-level model, we provide guidelines for formulating the operational schedule when the market operator is required to comply with the energy equity policy. This EESC-based relaxed model is essentially a distributed solution to the tie-line scheduling at the R-end, and of course, the S-end also needs to perform a regular ED each time, iteratively in accordance with the R-end.

B. Compact Formation of Proposed Model

After introducing the details of the proposed model, the corresponding compact model in vector form is given in this subsection for the convenience of discussing the solution methodology. It is important to note that we have ignored time stamps in the vector model because all the constraints are satisfied in every time slot, except the energy equity constraint (24), which is the constraint to the summation of daily energy cost.

$$\min_{\boldsymbol{y},\boldsymbol{P}}\left(\boldsymbol{a}^{\mathrm{T}}\boldsymbol{y}+\boldsymbol{c}^{\mathrm{T}}\boldsymbol{P}\right) \tag{17}$$

s.t.

$$\boldsymbol{BP}\leq\boldsymbol{d}\quad(\boldsymbol{\rho}) \tag{18}$$

$$\boldsymbol{Cy}\leq\boldsymbol{g} \tag{19}$$

$$\boldsymbol{y}+\mathbf{1}^{\mathrm{T}}\boldsymbol{P}=\mathbf{1}^{\mathrm{T}}\boldsymbol{D}\quad(\boldsymbol{\lambda}) \tag{20}$$

$$\boldsymbol{Gy}+\boldsymbol{JP}+\boldsymbol{HD}\leq\boldsymbol{f}\quad(\boldsymbol{\mu}) \tag{21}$$

$$\boldsymbol{y}\in\Phi \tag{22}$$

$$\Phi:=\left\{\boldsymbol{y}\;\middle|\;\min_{\boldsymbol{\lambda},\boldsymbol{\mu},\boldsymbol{s}}\mathbf{1}^{\mathrm{T}}\boldsymbol{s}=\mathbf{0},\ \text{s.t.}\,(24)\text{-}(30)\right\} \tag{23}$$

$$\left(\boldsymbol{\lambda}^{\mathrm{T}}\circ\mathbf{1}^{\mathrm{T}}+\boldsymbol{\mu}^{\mathrm{T}}\boldsymbol{H}+\boldsymbol{s}^{\mathrm{T}}\right)\boldsymbol{D}\leq ec^{thd} \tag{24}$$

$$\boldsymbol{Ls}\leq\boldsymbol{h} \tag{25}$$

$$\boldsymbol{\lambda},\boldsymbol{\mu}\in\Theta \tag{26}$$

$$\Theta:=\left\{(18),\,(20),\,(21),\,(28)\text{-}(30)\right\} \tag{27}$$

$$\boldsymbol{BP}+\boldsymbol{K}_{\rho}\boldsymbol{\rho}+\boldsymbol{M}_{\rho}\boldsymbol{z}_{\rho}\leq\boldsymbol{b}_{\rho} \tag{28}$$

$$\boldsymbol{Gy}+\boldsymbol{JP}+\boldsymbol{K}_{\mu}\boldsymbol{\mu}+\boldsymbol{M}_{\mu}\boldsymbol{z}_{\mu}\leq\boldsymbol{b}_{\mu} \tag{29}$$

$$\boldsymbol{c}^{\mathrm{T}}+\boldsymbol{\rho}^{\mathrm{T}}\boldsymbol{B}+\boldsymbol{\lambda}^{\mathrm{T}}\mathbf{1}^{\mathrm{T}}+\boldsymbol{\mu}^{\mathrm{T}}\boldsymbol{J}=\mathbf{0} \tag{30}$$

In the objective function (17), $\boldsymbol{y}$ is the vector of the tie-line energy variables. Constraint (18) is related to (2), wherein $\boldsymbol{d}$ is the right-side term after the rearrangement. Constraint (19) comes from the tie-line energy capacity limits given by (3). Constraint (20) is the energy balance constraint extracted from (4), where $\mathbf{1}$ is the column vector, and is regulated as $\mathbf{1}_n=[1,1,\ldots,1]\in\mathbb{R}^n$, and $\boldsymbol{D}$ is the vector of load with the consideration of renewable energy compensation (equivalent to a negative load). Constraint (21) is related to power flow constraints. Constraints (24) and (25) denote the constraints for the EESC variable derived from (9) and (10), wherein the notation "$\circ$" is the Hadamard product. Constraint (26) indicates that the LMP variables are determined by Θ. Constraint (27) gives the primal feasibility conditions. Constraints (28) and (29) represent the complementarity slackness conditions. $\boldsymbol{K}$, $\boldsymbol{M}$, and $\boldsymbol{b}$ are the coefficients after rearranging constraints (13)-(15). And (30) is derived from the stationarity constraints given in (16).

IV. Solution Methodology

A. Duality Theorem and Feasibility Cuts

In order to solve the bi-level model presented by (17)-(30) in Section III, we partition it into a master problem and a sub-problem. The master problem overlaps completely with the aforementioned upper-level model (17)-(22) with the exception that (22) is replaced by the proposed feasibility cuts, which are produced after solving the sub-problem based on the duality theorem. The detailed diagram of the solution algorithm is given in Section IV-C after the solution methodology is introduced.

1) Sub-problem

The sub-problem, denoted as S in this part, inherits the structure of the lower-level model (23)-(30), with the following modifications: ① the vector $\boldsymbol{y}$ is regarded as a right-side term to indicate the given purchased tie-line energy capacity; ② constraint (23) is relaxed to the objective function (31) by neglecting the "equals-to-0" requirement, but this feasibility will be ensured by the proposed feasibility cuts afterward; ③ the feasible set Θ is constructed to depict the feasible region determined by LMP variables, in which the constraints can be supplemented directly to the outer sub-problem. Hence, the sub-problem is first formulated as problem S in (31) and (32).

$$\min_{\boldsymbol{P},\boldsymbol{\rho},\boldsymbol{\lambda},\boldsymbol{\mu},\boldsymbol{s}} S=\mathbf{1}^{\mathrm{T}}\boldsymbol{s} \tag{31}$$

s.t.

$$\begin{cases}\left(\boldsymbol{\lambda}^{\mathrm{T}}\circ\mathbf{1}^{\mathrm{T}}+\boldsymbol{\mu}^{\mathrm{T}}\boldsymbol{H}+\boldsymbol{s}^{\mathrm{T}}\right)\boldsymbol{D}\leq ec^{thd}\\ \boldsymbol{Ls}\leq\boldsymbol{h}\\ \boldsymbol{BP}\leq\boldsymbol{d}\\ \mathbf{1}^{\mathrm{T}}\boldsymbol{P}=\mathbf{1}^{\mathrm{T}}\boldsymbol{D}-\boldsymbol{y}\\ \boldsymbol{JP}\leq\boldsymbol{f}-\boldsymbol{HD}-\boldsymbol{Gy}\\ \boldsymbol{BP}+\boldsymbol{K}_{\rho}\boldsymbol{\rho}+\boldsymbol{M}_{\rho}\boldsymbol{z}_{\rho}\leq\boldsymbol{b}_{\rho}\\ \boldsymbol{JP}+\boldsymbol{K}_{\mu}\boldsymbol{\mu}+\boldsymbol{M}_{\mu}\boldsymbol{z}_{\mu}\leq\boldsymbol{b}_{\mu}-\boldsymbol{Gy}\\ \boldsymbol{c}^{\mathrm{T}}+\boldsymbol{\rho}^{\mathrm{T}}\boldsymbol{B}+\boldsymbol{\lambda}^{\mathrm{T}}\mathbf{1}^{\mathrm{T}}+\boldsymbol{\mu}^{\mathrm{T}}\boldsymbol{J}=\mathbf{0}\end{cases} \tag{32}$$

Sub-problem S is formulated as a mixed-integer linear programming (MILP) problem, and algorithms such as Benders decomposition [43] and column-and-constraint generation (C&CG) [44] can be directly applied to solve it. However, S is a relaxed problem because it neglects the constraint $\mathbf{1}^{\mathrm{T}}\boldsymbol{s}=\mathbf{0}$ in (23). In other words, if the objective value of the solution is larger than $\mathbf{0}$, the original lower-level model is infeasible. Therefore, in this part, we propose feasibility cuts based on the duality theorem to prune the undesired feasible region in the master problem as follows. After obtaining the results of binary variables $\boldsymbol{z}_{\rho}$ and $\boldsymbol{z}_{\mu}$, we substitute them back into problem S, thereby reformulating S as a linear program (LP) problem, which we will refer to as S'.

$$\min_{\boldsymbol{P},\boldsymbol{\rho},\boldsymbol{\lambda},\boldsymbol{\mu},\boldsymbol{s}} S'=\mathbf{1}^{\mathrm{T}}\boldsymbol{s} \tag{33}$$

s.t.

$$\begin{cases}\left(\boldsymbol{\lambda}^{\mathrm{T}}\circ\mathbf{1}^{\mathrm{T}}+\boldsymbol{\mu}^{\mathrm{T}}\boldsymbol{H}+\boldsymbol{s}^{\mathrm{T}}\right)\boldsymbol{D}\leq ec^{thd}\quad(\boldsymbol{\delta})\\ \boldsymbol{Ls}\leq\boldsymbol{h}\quad(\boldsymbol{\varepsilon})\\ \boldsymbol{BP}\leq\boldsymbol{d}\quad(\boldsymbol{\varphi})\\ \mathbf{1}^{\mathrm{T}}\boldsymbol{P}=\mathbf{1}^{\mathrm{T}}\boldsymbol{D}-\boldsymbol{y}\quad(\boldsymbol{\gamma})\\ \boldsymbol{JP}\leq\boldsymbol{f}-\boldsymbol{HD}-\boldsymbol{Gy}\quad(\boldsymbol{\eta})\\ \boldsymbol{BP}+\boldsymbol{K}_{\rho}\boldsymbol{\rho}\leq\boldsymbol{b}_{\rho}-\boldsymbol{M}_{\rho}\bar{\boldsymbol{z}}_{\rho}\quad(\boldsymbol{\pi})\\ \boldsymbol{JP}+\boldsymbol{K}_{\mu}\boldsymbol{\mu}\leq\boldsymbol{b}_{\mu}-\boldsymbol{Gy}-\boldsymbol{M}_{\mu}\bar{\boldsymbol{z}}_{\mu}\quad(\boldsymbol{\sigma})\\ \boldsymbol{c}^{\mathrm{T}}+\boldsymbol{\rho}^{\mathrm{T}}\boldsymbol{B}+\boldsymbol{\lambda}^{\mathrm{T}}\mathbf{1}^{\mathrm{T}}+\boldsymbol{\mu}^{\mathrm{T}}\boldsymbol{J}=\mathbf{0}\quad(\boldsymbol{\zeta})\end{cases} \tag{34}$$

The preceding introduction to the lower level of the proposed model demonstrates its responsibility for evaluating the typical characteristics of the energy burden violation based on the given operational schedule. In the solution methodology, this violation is illustrated by the EESC variable $\boldsymbol{s}$ and is thereby regulated to be 0. Consequently, we obtain the dual problem of S', denoted as R in (35) and (36), and the duality theorem is adopted to evaluate the desired adjustments to the operational schedule because of the energy burden violation.

$$\begin{aligned}\max_{\delta,\varepsilon,\varphi,\gamma,\eta,\pi,\sigma,\zeta} R = & ec^{thd}\cdot\boldsymbol{\delta}+\boldsymbol{h}^{\mathrm{T}}\boldsymbol{\varepsilon}+\boldsymbol{d}^{\mathrm{T}}\boldsymbol{\varphi}+\left(\mathbf{1}^{\mathrm{T}}\boldsymbol{D}-\boldsymbol{y}\right)^{\mathrm{T}}\boldsymbol{\gamma}+\\ & \left(\boldsymbol{f}-\boldsymbol{HD}-\boldsymbol{Gy}\right)^{\mathrm{T}}\boldsymbol{\eta}+\left(\boldsymbol{b}_{\rho}-\boldsymbol{M}_{\rho}\bar{\boldsymbol{z}}_{\rho}\right)^{\mathrm{T}}\boldsymbol{\pi}+\\ & \left(\boldsymbol{b}_{\mu}-\boldsymbol{Gy}-\boldsymbol{M}_{\mu}\bar{\boldsymbol{z}}_{\mu}\right)^{\mathrm{T}}\boldsymbol{\sigma}\end{aligned} \tag{35}$$

s.t.

$$\begin{cases}\boldsymbol{B}^{\mathrm{T}}\left(\boldsymbol{\varphi}+\boldsymbol{\pi}\right)+\mathbf{1}\circ\boldsymbol{\gamma}+\boldsymbol{J}^{\mathrm{T}}\left(\boldsymbol{\eta}+\boldsymbol{\sigma}\right)=\mathbf{0}\\ \boldsymbol{K}_{\rho}^{\mathrm{T}}\boldsymbol{\pi}+\boldsymbol{B\zeta}=\mathbf{0}\\ \boldsymbol{D\delta}+\boldsymbol{\zeta}=\boldsymbol{0}\\ \boldsymbol{H\delta}+\boldsymbol{K}_{\mu}^{\mathrm{T}}\boldsymbol{\sigma}+\boldsymbol{J\zeta}=\mathbf{0}\\ \boldsymbol{D\delta}+\boldsymbol{L}^{\mathrm{T}}\boldsymbol{\varepsilon}=\mathbf{1}^{\mathrm{T}}\end{cases} \tag{36}$$

As problem S' is an LP, the solved objective value of primal problem S' equals that of the dual problem R under strong duality. In simpler terms, when the sub-problem is infeasible ($\mathbf{1}^{\mathrm{T}}\boldsymbol{s}>\mathbf{0}$), it is equivalent to the objective value of a dual problem (35), i.e., larger than 0. If we denote R_k as the optimal solution of problem R in the k^{th} iteration, based on the previous discussion on infeasibility, it could be concluded that $R_k>0$ corresponds to the feasible region in the master problem that would cause the infeasibility of sub-problems (31) and (32). Conversely, the constraint $R_k\leq 0$ is able to cut off the related feasible region. The same can be illustrated from the model perspective: when the solved optimal purchased tie-line energy is given from the master problem to the sub-problem, the threshold of the energy cost will be exceeded. Consequently, in the k^{th} iteration, a feasibility cut (37) is proposed to gradually prune the feasible region in the master problem for the purpose of ensuring the feasibility of the sub-problem in the next iteration.

$$\begin{aligned}R_k = & ec^{thd}\cdot\boldsymbol{\delta}_k+\boldsymbol{h}^{\mathrm{T}}\boldsymbol{\varepsilon}_k+\boldsymbol{d}^{\mathrm{T}}\boldsymbol{\varphi}_k+\left(\mathbf{1}^{\mathrm{T}}\boldsymbol{D}-\boldsymbol{y}\right)^{\mathrm{T}}\boldsymbol{\gamma}_k+\\ & \left(\boldsymbol{f}-\boldsymbol{HD}-\boldsymbol{Gy}\right)^{\mathrm{T}}\boldsymbol{\eta}_k+\left(\boldsymbol{b}_{\rho}-\boldsymbol{M}_{\rho}\bar{\boldsymbol{z}}_{\rho}\right)^{\mathrm{T}}\boldsymbol{\pi}_k+\\ & \left(\boldsymbol{b}_{\mu}-\boldsymbol{Gy}-\boldsymbol{M}_{\mu}\bar{\boldsymbol{z}}_{\mu}\right)^{\mathrm{T}}\boldsymbol{\sigma}_k\leq 0\end{aligned} \tag{37}$$

2) Master Problem

With the supplement of the feasibility cuts, the master problem in the k^{th} iteration is constructed, with objective function in (17) and constraints as (18)-(21) and (38).

$$\begin{aligned}& ec^{thd}\cdot\boldsymbol{\delta}_l+\boldsymbol{h}^{\mathrm{T}}\boldsymbol{\varepsilon}_l+\boldsymbol{d}^{\mathrm{T}}\boldsymbol{\varphi}_l+\left(\mathbf{1}^{\mathrm{T}}\boldsymbol{D}-\boldsymbol{y}\right)^{\mathrm{T}}\boldsymbol{\gamma}_l+\\ & \left(\boldsymbol{f}-\boldsymbol{HD}-\boldsymbol{Gy}\right)^{\mathrm{T}}\boldsymbol{\eta}_l+\left(\boldsymbol{b}_{\rho}-\boldsymbol{M}_{\rho}\bar{\boldsymbol{z}}_{\rho}\right)^{\mathrm{T}}\boldsymbol{\pi}_l+\\ & \left(\boldsymbol{b}_{\mu}-\boldsymbol{Gy}-\boldsymbol{M}_{\mu}\bar{\boldsymbol{z}}_{\mu}\right)^{\mathrm{T}}\boldsymbol{\sigma}_l\leq\mathbf{0}\quad\forall l\leq k\end{aligned} \tag{38}$$

It is worth noting that (38) is a set of explicit constraints of vector $\boldsymbol{y}$, i.e., the proposed feasibility cuts convert the implicit energy equity constraints into the explicit supplementary constraints of the tie-line energy purchase plan. By leveraging the proposed EESC variable, the social-driven locational price constraints are relaxed, and the typical violation characteristics in the sub-problem are obtained based on the duality theorem.

B. Subsidy Policy and Convergence Acceleration

Up to this point, we have introduced the tie-line scheduling solution when the requirements from energy equity policies are given to the market operators. However, the operational schedule may vary when given different energy cost thresholds, and the model may even be infeasible if the energy burden threshold is too tight. Hence, in this subsection, we further formulate the subsidy policy guidelines for the proposed tie-line scheduling model by necessary modifications. For the constraint (9) in the sub-problem, if we expand the sum within the parentheses, the second term $\sum es_{n^{eb}t}\cdot P_{d(n^{eb})t}$ will be the production of the EBSC variable and the nodal load capacity. As the EBSC variable is supposed to be the slack LMP for the energy burden-suffering node, this production happens to equal the potential subsidies that the market operator must provide to the users, when the given operational schedule is not able to meet the energy equity requirement. Therefore, the original objective function of sub-problem (31) is consistent with minimizing the subsidy $\boldsymbol{D}^{\mathrm{T}}\boldsymbol{s}$, as $\boldsymbol{D}$ is considered inelastic in the proposed model. Note that in the objective function (17) of the master problem, the cost of the subsidy has not been considered; therefore, the subsidy variable $\alpha\in\mathbb{R}^{1\times 1}$ is added to the objective function, and (17) is modified as (39).

$$\min_{\boldsymbol{y},\boldsymbol{P},\alpha}\left(\boldsymbol{a}^{\mathrm{T}}\boldsymbol{y}+\boldsymbol{c}^{\mathrm{T}}\boldsymbol{P}+\alpha\right) \tag{39}$$

According to the conclusions in [45] and [46], optimality cuts are more effective than feasibility cuts in the iteration. Therefore, based on the theory of Benders decomposition and C&CG algorithms [43], [44], we develop the optimality cuts (40) by modifying feasibility cuts (38).

$$\begin{aligned}\alpha\geq & ec^{thd}\cdot\boldsymbol{\delta}_l+\boldsymbol{h}^{\mathrm{T}}\boldsymbol{\varepsilon}_l+\boldsymbol{d}^{\mathrm{T}}\boldsymbol{\varphi}_l+\left(\mathbf{1}^{\mathrm{T}}\boldsymbol{D}-\boldsymbol{y}\right)^{\mathrm{T}}\boldsymbol{\gamma}_l+\\ & \left(\boldsymbol{f}-\boldsymbol{HD}-\boldsymbol{Gy}\right)^{\mathrm{T}}\boldsymbol{\eta}_l+\left(\boldsymbol{b}_{\rho}-\boldsymbol{M}_{\rho}\bar{\boldsymbol{z}}_{\rho}\right)^{\mathrm{T}}\boldsymbol{\pi}_l+\\ & \left(\boldsymbol{b}_{\mu}-\boldsymbol{Gy}-\boldsymbol{M}_{\mu}\bar{\boldsymbol{z}}_{\mu}\right)^{\mathrm{T}}\boldsymbol{\sigma}_l\quad\forall l\leq k\end{aligned} \tag{40}$$

$\left(\boldsymbol{y}_k,\boldsymbol{P}_k,\alpha_k\right)$ is the current solution of the master problem, and the consequent objective solution of the sub-problem given $\boldsymbol{y}_k$ is denoted as $\boldsymbol{s}_k$. If $\alpha_k<\boldsymbol{D}^{\mathrm{T}}\boldsymbol{s}_k$, then in each iteration, we repeatedly add (40) into the master problem to cut off the feasible region that corresponds to the solution $\left(\boldsymbol{y}_k,\boldsymbol{P}_k,\alpha_k\right)$.

C. Algorithm of Solution Methodology

In conclusion, the algorithm for solving the proposed model with subsidy policy is shown in Algorithm 1.

The bi-level structure of the proposed model is also illustrated in Fig. 2, where the upper level sends the tie-line energy variables to the lower level, and all the dual variables are sent from the lower level to formulate the feasibility cuts.

Due to space limitations and for clarity, some details of the model and solution methodology have not been illustrated, and we acknowledge these details in this subsection.

Algorithm 1: duality theorem-based algorithm with improved feasibility cuts

1 Set the iteration index $k=1$, energy burden constraint threshold eb^{thd}, and convergence criterion ϵ. Initialize the tie-line energy purchase plan $\boldsymbol{y}_k$ and operational schedule $\boldsymbol{P}_k$, receive the S-end asking price of tie-line energy $\boldsymbol{a}^{\mathrm{T}}$, and set the initial subsidy $\alpha_k=0$

2 Set the upper bound of the proposed model as $UB=+\infty$, and lower bound as $LB=\boldsymbol{a}^{\mathrm{T}}\boldsymbol{y}_k+\boldsymbol{c}^{\mathrm{T}}\boldsymbol{P}_k+\alpha_k$

3 **Repeat**

4 Solve the sub-problem $S\left(\min \mathbf{1}^{\mathrm{T}}\boldsymbol{s}\right)$ (31) with the constraints (32), and obtain the optimal solution $\boldsymbol{s}_k$. Update $UB=\boldsymbol{a}^{\mathrm{T}}\boldsymbol{y}_k+\boldsymbol{c}^{\mathrm{T}}\boldsymbol{P}_k+\boldsymbol{D}^{\mathrm{T}}\boldsymbol{s}_k$

5 By fixing the outcoming results of binary variables $\boldsymbol{z}_\rho$ and $\boldsymbol{z}_\mu$, the problem S is transformed into LP problem S' in (33) and (34)

6 Based on strong duality, convert the LP problem S' to its dual form R in (35) and (36), solve the problem R, and obtain the solution in the k^{th} iteration: $\left(\boldsymbol{\delta}_k,\boldsymbol{\varepsilon}_k,\boldsymbol{\varphi}_k,\boldsymbol{\gamma}_k,\boldsymbol{\eta}_k,\boldsymbol{\pi}_k,\boldsymbol{\sigma}_k,\boldsymbol{\zeta}_k\right)$

7 Solve the master problem $\min\left(\boldsymbol{a}^{\mathrm{T}}\boldsymbol{y}+\boldsymbol{c}^{\mathrm{T}}\boldsymbol{P}+\alpha\right)$ in (39), subjected to constraints (18) - (21), and add the additional improved feasibility cut (40)

8 Obtain the solution, denoted as $\left(\boldsymbol{y}_{k+1},\boldsymbol{P}_{k+1},\alpha_{k+1}\right)$, and update $LB=\boldsymbol{a}^{\mathrm{T}}\boldsymbol{y}_{k+1}+\boldsymbol{c}^{\mathrm{T}}\boldsymbol{P}_{k+1}+\alpha_{k+1}$

9 $k=k+1$

10 **Until** $|UB-LB|<\epsilon$, then submit the tie-line energy purchase plan $\boldsymbol{y}$ to the S-end

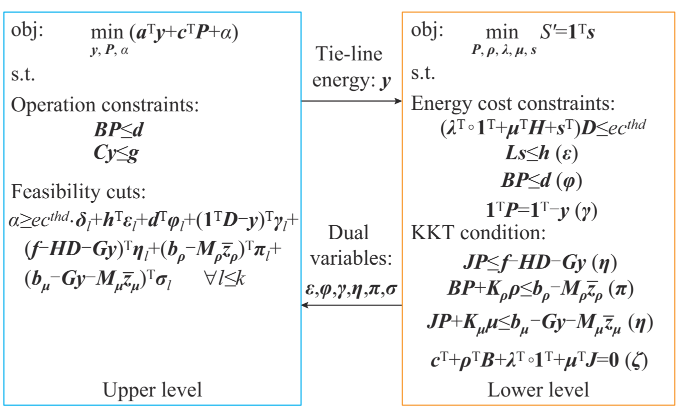

Fig. 2. Schematic diagram of bi-level structure of proposed model.

D. Additional Remarks

1) In the modified objective function (39), it is noteworthy that the subsidy term has the same unit with operational cost as "\$", so there is no need to assign a weight coefficient for α, and thus no optimality gap will be introduced in the proposed model.

2) After solving the proposed model with the solution methodology, the market operator of the R-end submits the current energy purchase plan to the S-end. Then, the S-end will update the offering price based on its own supply curve, and the R-end will develop the tie-line schedule iteratively until the multi-area market is cleared. In the proposed model, we adopt the classical alternating direction method of multipliers (ADMM) [47], which is not specified in the mathematical model for simplicity. According to the widely studied distributed algorithms, the method is scalable for circumstances with multiple R-ends.

3) For the cost function of generators in (1), we adopt the simplified form of the linear function. Nevertheless, when concentrating on the distributed clearing market, to enhance the convergence of the regional market clearing process, quadratic economic function (with piece-wise-linear technology employed) is introduced in some models to ensure that the supply curves of both market participants are sloping. There are also many other equivalent and tighter convex forms for the cost function and the constraints in the UC and ED problems. Please refer to [48] and [49] for more details.

4) In the numerical simulation section (Section V), to further facilitate the iteration efficiency, we also make modifications to the market information submitted by both participants in (41), wherein subscript i is the iteration index between S-end and R-end when clearing the distributed market (be sure to distinguish from the tie-line scheduling iteration within the R-end). Correction coefficients τ^p and τ^c vary from $[0,\ 1]$ to modify $\boldsymbol{a}^{\mathrm{T}}$ and the purchase plan $\boldsymbol{y}$, respectively.

$$\begin{cases}\boldsymbol{y}_{i+1}=\left(\boldsymbol{y}_{i+1}-\boldsymbol{y}_i\right)\tau^p\\ \boldsymbol{a}_{i+1}=\left(\boldsymbol{a}_{i+1}-\boldsymbol{a}_i\right)\tau^c\end{cases} \tag{41}$$

5) Considering that we are focusing on the constraints for locational price in the systems, it should be noted that the negative nodal price may occur in some extreme circumstances, especially when renewable energy generators participate in bidding. However, in the proposed model, we focus on the total energy cost of certain buses, and the negative prices are unlikely to occur at load buses.

6) The uncertainties of renewable energy resources are not specifically considered in this paper because we want to salient the inter-area trading mechanism with energy equity constraints. However, it is easy to enforce them with robust or stochastic methods, which are also parts of our future works.

V. Computational Results

In the simulation, we first apply the proposed model and solution methodology to the smaller test systems consisting of two and three Pennsylvania-New Jersey-Maryland (PJM) 5-bus systems, then adopt the larger Northeast Power Coordinating Council (NPCC) test system to validate the effectiveness of the proposed tie-line scheduling model with energy equity constraints.

A. Two PJM 5-bus Interconnected Test System

The test system in this subsection, as shown in Fig. 3, consists of two PJM 5-bus systems, wherein Bus C of the S-end and Bus B of the R-end are connected by a 400 MW tie-line with 0.01 p.u. reactance, and in Bus A, the generator Park City is aggregated into Alta. The detailed economic data of both the generator and the network are taken from [50]. Consistent with the aforementioned presupposition, the energy equity policies are implemented on the R-end, wherein Bus C is assumed to be the aggregated node of low-income communities. Hence, the market operator in the R-end (Operator-R) will iteratively reformulate the daily tie-line energy purchase plan to obtain the desired system price pattern for the purpose of ensuring the energy expenditure of Bus C is within the given threshold. In Fig. 3, Operator-S represents the market operation in the S-end.

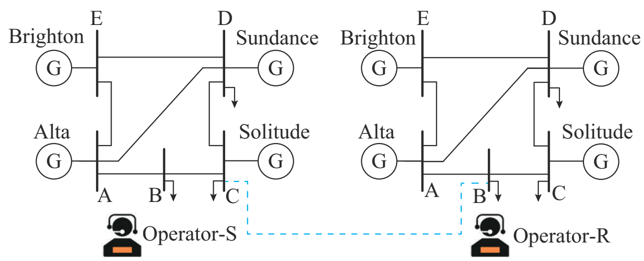

Fig. 3. Diagram of two PJM 5-bus test systems.

The operational horizon is set to be 24 hours with a one-hour resolution. After applying the proposed model and the solution methodology, the operational results under different required energy cost thresholds (ec^{thd}) are shown in Table I. Note that when ec^{thd} is $45000, the energy cost constraints are all unbinding in the model, indicating that the cases with ec^{thd} act as the benchmarks. In Table I, the S-end cost is the total cost of the sending area (tie-line export revenue subtracted from operation cost); the total cost is the cost of entire interconnected systems; the social cost is the incremental cost of our proposed operational scheme to the conventional economic-driven model; S-end generation and R-end generation are the total generation capacities within the operational horizon for S- and R-ends, respectively; and the exchange is the exchanging capacity on the tie-line.

TABLE I
ECONOMIC RESULTS OF OPERATIONAL SCHEDULES UNDER DIFFERENT ENERGY COST THRESHOLDS

ec^{thd} ($)	S-end cost ($)	R-end cost ($)			Total cost ($)	Social cost ($)	S-end generation (MWh)	R-end generation (MWh)	Exchange (MWh)
		Operation	Tie-line import	Subsidy					
45000	65665	66412	45875	0	177952		10365	6059	2853
43000	64393	59932	53907	0	178232	280	10782	5654	3258
41000	62219	52133	64761	0	179113	1161	11307	5119	3792
39000	61092	48284	70468	706	180550	2598	11606	4809	4103
37000	61092	48284	70468	2707	182551	4599	11606	4809	4103

With more intensified ec^{thd} from $45000 to $37000, the proposed tie-line schedule at the R-end gradually purchases more import tie-line energy from the S-end to reduce the local energy price, and consequently, the import cost increases from $45875 to $70468. Although the operational cost of the generation units is reduced from $66412 to $48284 accordingly, the total cost to the R-end is higher because of the stricter energy cost threshold requirement. When the threshold ec^{thd} is as low as $39000, the market operator has to provide a subsidy to the concentrated community to limit the daily household energy expenditures within the social-driven cost constraints. It should also be noted that for the S-end, the ED cost (S-end cost plus trading revenue) also increases from $111540 to $131560 due to the larger energy demand at the R-end. We can therefore conclude that the S-end also contributes partly to the implementation of the energy equity requirements, while still ensuring information privacy, as it only requires the exchange of boundary information. When ec^{thd} is set as $45000, the social-driven locational cost constraints will not make any additional impact on the operational schedule, i.e., the constraints are unbinding to the problem. Conversely, if the threshold ec^{thd} is lower than $37000, purely adjusting the energy purchase plan and operational schedule will make no difference to the nodal energy prices, and a higher subsidy is the only effective solution to implement the energy equity policy.

For a more specific illustration, the cleared tie-line energy purchase plan and cleared price are shown in Table II, which reveals that with stricter energy equity constraints, even when the cleared price of tie-line energy is growing, the energy price of bus n^{eb} may still decrease under our proposed tie-line schedule. We also compare the system-wide daily total energy expenditure in Table II to evaluate the social welfare acquired by the proposed model. As illustrated, the total energy expenditure at the S-end is lower than that at the R-end in the benchmark case (ec^{thd} of $45000). When the energy burden constraints at the R-end get tighter, the total energy expenditure at the R-end gets lower and reversely at the S-end. The total energy expenditure of the two-area system keeps decreasing till the energy cost constraints are saturated. As a result, the proposed model relieves the total energy expenditure of the users in the interconnected system, and thereby enhances the system-wide social welfare.

TABLE II
CLEARED TIE-LINE ENERGY PURCHASE PLAN, CLEARED PRICES, AND SOCIAL WELFARE

ec^{thd} ($)	Tie-line energy (MW)	Cleared price ($/MW)	LMP of bus n^{ec} ($/MW)	S-end expense (10^3 $)	R-end expense (10^3 $)	Total energy expenditure (10^3 $)
45000	149.48	11.14	11.14	134.0	149.2	283.2
43000	151.28	11.76	11.11	137.1	143.3	280.4
41000	186.47	12.09	10.50	141.4	136.3	277.7
39000	215.38	12.39	9.99	143.2	132.3	275.5
37000	215.38	12.39	9.99	143.2	132.3	275.5

The iteration between the areas is explained by the updated supply curves of the R-end, as shown in Fig. 4. According to the gradually added optimality cuts introduced by (40), the structure of the ED problem for the R-end varies in each iteration, as shown in Fig. 4(a), wherein $R^{(i)}$ is the supply curve in the i^{th} information exchange between the S-end and R-end. Therefore, the model is more flexible compared with the fixed supply curve, though of course, with a heavier computational burden. Further, the detailed curves for the R-end when ec^{thd} is \$41000 are represented in Fig. 4(b), wherein the S-end supply curve is omitted for clarity. Different colors of the curves represent different iterations. The spots and the trajectory in the figure are the iteratively evolving solutions to the problem, and ultimately, spot P is the optimal solution with tie-line energy of 186.47 MW and a cleared price of 12.09 \$/MW, consistent with the results in Table II. It is obvious that only the varying curves can ensure enough flexibility in searching for the optimal solution when restricted by the embedded energy equity constraints.

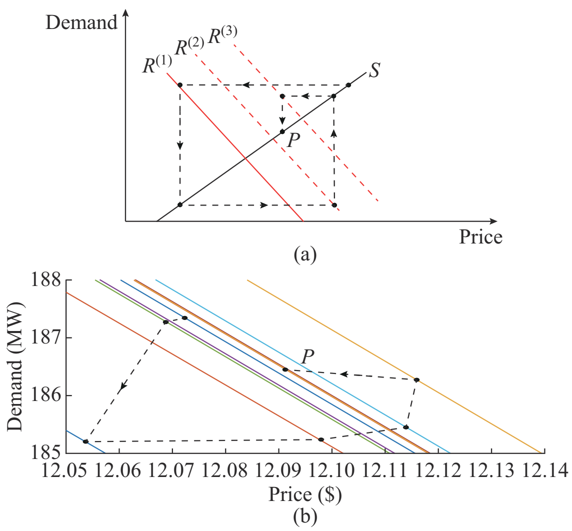

Fig. 4. Updated supply curves of R-end. (a) Curves in each iteration. (b) Detailed curves when ec^{thd} is \$41000.

To verify the sustainability of the proposed model, we further compare the conventional coupon-based models and the proposed model, and the economic results are given in Table III. It is shown that at each level of energy cost requirement, the social cost (e. g., the policy cost) is always lower than the straightforward coupon cost. This is because the systematically optimal solution is explored by the proposed model, and therefore, this novel utility model is more sustainable than the conventional payment assistance programs.

TABLE III
COMPARISON BETWEEN COUPON-BASED MODEL AND PROPOSED MODEL

ec^{thd} (\$)	Total cost (\$)	Social cost (\$)	Coupon cost (\$)
45000	177952		
43000	178232	280	2000
41000	179113	1161	4000
39000	180550	2598	6000
37000	182551	4599	8000

The support from the S-end is illustrated in Fig. 5, wherein the output of generators at the S-end with different energy cost thresholds (ec^{thd}) are presented. With stricter energy equity constraints (lower threshold) at the R-end, the output of generators at the S-end generally increases. It should be noted that the generation cost at the S-end increases due to the new tie-line schedule of the R-end, namely, the S-end will indirectly provide support to the R-end when participating in this market. This conclusion is consistent with the previous assumption that directly adding the social-driven cost constraints into the ED problem of the R-end is not a valid method for formulating the desired operational schedule. Rather, the implementation of energy equity policies needs support from the whole system.

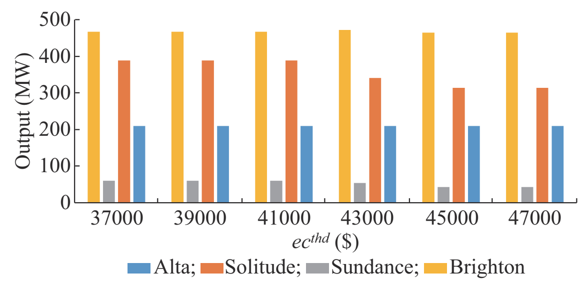

Fig. 5. Output of generators at S-end with different ec^{thd}.

B. Three PJM 5-bus Interconnected Test System

In this subsection, we apply the proposed model to a three PJM 5-bus interconnected test system to verify its scalability. The schematic diagram of the supplementary case study is shown in Fig. 6, and the economic results are also presented and analyzed in Table IV. In this case, the S-end is interconnected with R-end #1 and R-end #2 by two tie-lines. The energy burden policy is only implemented into R-end #1, which means that only Operator-R1 needs to develop a novel utility model to embed the social-driven energy cost constraints.

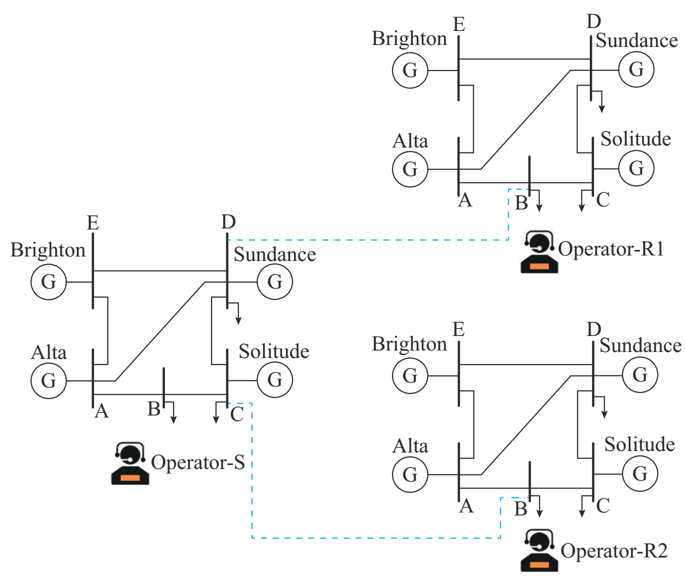

Fig. 6. Diagram of three PJM 5-bus interconnected test system.

TABLE IV
ECONOMIC RESULTS OF THREE PJM 5-BUS INTERCONNECTED TEST SYSTEMS

ec^{thd} ($)	S-end cost ($)	R-end #1 cost ($)			R-end #2 cost ($)		Total cost ($)
		Operation	Tie-line import	Subsidy	Operation	Tie-line import	
45000	67608	66884	45479	0	72572	12691	265234
43000	66336	60404	53511	0	72969	12884	266104
41000	64162	52605	64365	0	73681	12913	267726
39000	63035	48756	70072	791	74773	13206	270633
37000	63035	48756	70072	2792	74773	13206	272634

It is illustrated in Table IV that the stricter the requirements of the energy burden threshold, the higher the demand for the R-end #1. This is because the R-end #1 needs to import more tie-line energy to regulate its price pattern. On the other side, the updated settlement point increases the export tie-line price at the S-end, and the cost of R-end #2 still gets higher, even without energy burden requirements in this area.

C. Two NPCC 140-bus Test Systems

Following the application of the proposed model to the smaller test system, in this subsection, we apply the proposed model to a larger system, consisting of two NPCC 140-bus test systems, to validate the scalability of the model. The detailed network data is drawn from [51], and the system diagram is created with Another Grid Visualizer (AGVis) in [52], which is the visualization package of the CURENT Large-scale Testbed (LTB) [53].

In this test system, the low-income bus is Bus 114, and the energy price is higher due to congestion in transmission line 116 (buses 90-114). After implementing different energy cost thresholds on the proposed tie-line scheduling model, the market clearing results are shown in Table V.

TABLE V
MARKET CLEARING RESULTS OF DIFFERENT LOW-INCOME COMMUNITIES ENERGY COSTS

ec^{thd} (10^6 $)	S-end cost (10^6 $)	R-end cost (10^6 $)			Total cost (10^6 $)	Social cost (10^6 $)	S-end generation (GWh)	R-end generation (GWh)	Exchange (GWh)
		Operation	Tie-line import	Subsidy					
1.00	4.799	4.472	2.866	0	12.137		314.17	297.46	24.45
0.97	4.726	4.466	2.945	0	12.138	0.001	314.68	296.95	24.96
0.94	4.671	4.461	3.011	0	12.143	0.006	315.30	396.33	25.58
0.91	4.597	4.456	3.101	0	12.154	0.017	315.89	295.74	26.17
0.88	4.541	4.439	3.189	0.017	12.186	0.049	316.58	295.05	26.86

The results in Table V validate that the proposed model is also effective for the larger test system when following the same trend as discussed in this paper. In Fig. 7, system price patterns with and without social-driven cost constraints are depicted and illustrated using a reference price of 30 $/MW, and the proposed model is validated as successfully modulating the price pattern to a lower level.

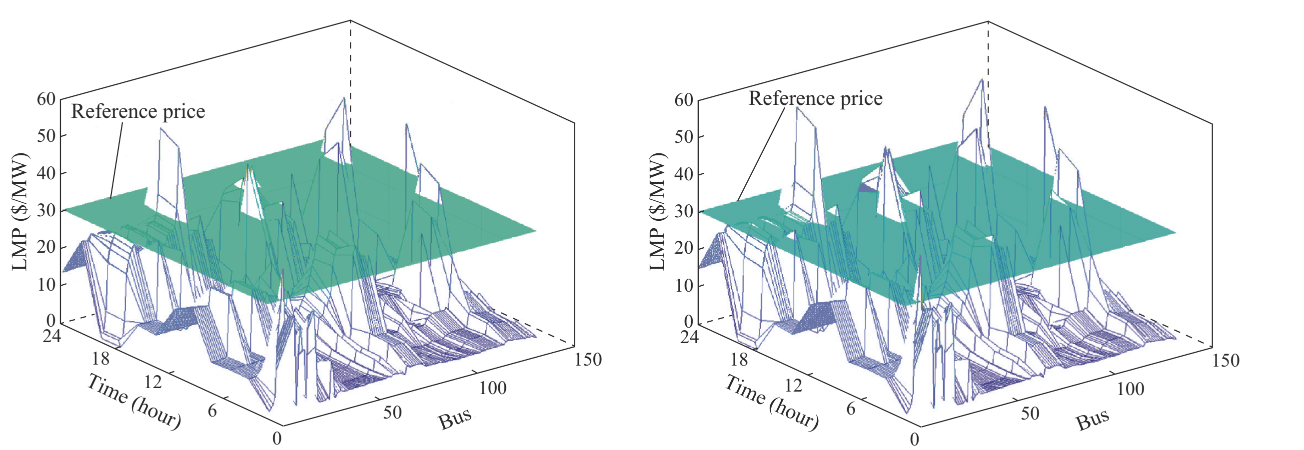

(a) (b)

Fig. 7. Energy price patterns with and without social-driven cost constraints. (a) With social-driven cost constraints. (b) Without social-driven cost constraints.

VI. Conclusion and Expectation

In this paper, we propose a novel bi-level energy equity-constrained tie-line scheduling model for interconnected systems to characterize the concept of energy equity, and develop technical implementation schemes for potential energy burden policies. The proposed model evaluates the gap between the given operational schedule and the desired equity-constrained schedule. The proposed model also provides guidelines to market operators for how to develop tie-line schedules as price takers to achieve the desired energy price pattern. Further, a subsidy policy is adopted in the proposed model by leveraging the improved optimality cuts, along with the duality theorem. In the case studies, the effectiveness of the proposed model is validated by the impact of the energy equity implementation, and the cost of meeting the requirements of energy equity is verified to be higher. In the future, we plan to further study energy equity by considering energy storage device planning problems under renewable energy uncertainty.

References

[1] S. Carley and D. M. Konisky, "The justice and equity implications of the clean energy transition," *Nature Energy*, vol. 5, no. 8, p. 8, Aug. 2020.

[2] K. E. Jenkins, B. K. Sovacool, N. Mouter *et al.*, "The methodologies, geographies, and technologies of energy justice: a systematic and comprehensive review," *Environmental Research Letters*, vol. 16, no. 4, p. 043009, Apr. 2021.

[3] U.S. Department of Energy. (2024, May). Low-income community energy solutions. [Online]. Available: https://www. energy. gov/scep/slsc/low-income-community-energy-solutions

[4] O. Ma, K. Laymon, M. H. Day *et al.*, "Low-income energy affordability data (LEAD) tool methodology," Tech. Rep., No. NREL/TP-6A20-74249, National Renewable Energy Laboratory, Golden, USA, Jul. 2019.

[5] K. Jenkins, D. McCauley, R. Heffron *et al.*, "Energy justice: a conceptual review," *Energy Research & Social Science*, vol. 11, pp. 174-182, Jan. 2016.

[6] C. Farley, J. Howat, J. Bosco *et al.* (2021, Nov.). Advancing equity in utility regulation. [Online]. Availbale: https://escholarship. org/content/qt1mr715sx/qt1mr715sx.pdf

[7] R. Day, G. Walker, and N. Simcock, "Conceptualising energy use and energy poverty using a capabilities framework," *Energy Policy*, vol. 93, pp. 255-264, Jun. 2016.

[8] U. S. Department of Energy. (2024, May). Weatherization Assistance Program (WAP). [Online]. Available: https://www.energy.gov/scep/wap/about-weatherization-assistance-program

[9] U. S. Department of Health and Human Services. (2024, May). Low Income Home Energy Assistance Program (LIHEAP). [Online]. Available: https://www.acf.hhs.gov/ocs /programs/liheap

[10] BBC News. (2023, Aug). French government limits electricity price rises. [Online]. Available: https://www. bbc. com/news/business-60112068.

[11] The Local. (2022, Jan.). Denmark could give tax-free sum to families with high heating bills. [Online]. Available: https://www. thelocal. dk/20220127/ denmark-could-give-tax-free-sum-to-families-with-high-heating-bills

[12] UK Government. (2023, May). Energy price guarantee. [Online]. Available: https://www. gov. uk/government/publications/energy-bills-support/energy-bills-support-factsheet-8-september-2022

[13] T. Levin, J. Bistline, R. Sioshansi *et al.*, "Energy storage solutions to decarbonize electricity through enhanced capacity expansion modelling," *Nature Energy*, vol. 8, no. 11, pp. 1199-1208, Sept. 2023.

[14] M. Brown, A. Soni, M. Lapsa *et al.*, "Low-income energy affordability: conclusions from a literature review," Tech. Rep., No. ORNL/TM-2019/1150, Oak Ridge National Laboratory, Oak Ridge, USA, Mar. 2020.

[15] C. Li, F. Li, S. Jiang *et al.*, "Siting and sizing of DG units considering energy equity: model, solution, and guidelines," *IEEE Transactions on Smart Grid*, vol. 15, no. 4, pp. 3681-3693, Jul. 2024.

[16] A. Merzic, M. Music, and Z. Haznadar, "Conceptualizing sustainable development of conventional power systems in developing countries–a contribution towards low carbon future," *Energy*, vol. 126, pp. 112-123, May 2017.

[17] B. Tarekegne, D. Powell, K. Oikonomou *et al.*, "Analysis of energy justice and equity impacts from replacing peaker plants with energy storage," in *Proceedings of 2022 IEEE Electrical Energy Storage Application and Technologies Conference (EESAT)*, Austin, USA, Nov. 2022, pp. 1-5.

[18] Oregon State. (2021, Dec.). HB 3141. [Online]. Available: https://olis.oregonlegislature.gov/liz/2021R1/Measures/Overview/HB3141

[19] S. Michener, R. O'Neil, S. Atcitty *et al.*, "Energy storage for social equity roundtable report," Tech. Rep., No. PNNL-31964, Pacific Northwest National Laboratory, Tri-cities, USA, Sept. 2021.

[20] D. J. Bednar and T. G. Reames, "Recognition of and response to energy poverty in the United States," *Nature Energy*, vol. 5, no. 6, pp. 432-439, Mar. 2020.

[21] W. Gu and R. Sioshansi, "Market equilibria with energy storage as flexibility resources," *IEEE Open Access Journal of Power and Energy*, vol. 9, pp. 584-597, Nov. 2022.

[22] X. Fang and M. Cui, "Analytical model of day-ahead and real-time price correlation in strategic wind power offering," *Journal of Modern Power Systems and Clean Energy*, vol. 8, no. 5, pp. 1024-1027, Sept. 2020.

[23] Y. Du, F. Li, H. Zandi *et al.*, "Approximating Nash equilibrium in day-ahead electricity market bidding with multi-agent deep reinforcement learning," *Journal of Modern Power Systems and Clean Energy*, vol. 9, no. 3, pp. 534-544, May 2021.

[24] S. Liu, Y. Jiang, Z. Lin *et al.*, "Data-driven two-step day-ahead electricity price forecasting considering price spikes," *Journal of Modern Power Systems and Clean Energy*, vol. 11, no. 2, pp. 523-533, Mar. 2023.

[25] X. Fang, B.-M. Hodge, E. Du *et al.*, "Introducing uncertainty components in locational marginal prices for pricing wind power and load uncertainties," *IEEE Transactions on Power Systems*, vol. 34, no. 3, pp. 2013-2024, May 2019.

[26] X. Yang, C. Gu, X. Yan *et al.*, "Reliability-based probabilistic network pricing with demand uncertainty," *IEEE Transactions on Power Systems*, vol. 35, no. 5, pp. 3342-3352, Sept. 2020.

[27] H. Wang, Z. Bie, and H. Ye, "Locational marginal pricing for flexibility and uncertainty with moment information," *IEEE Transactions on Power Systems*, vol. 38, no. 3, pp. 2761-2775, May 2023.

[28] A. Campbell, "Cap prices or cap revenues? The dilemma of electric utility networks," *Energy Economics*, vol. 74, pp. 802-812, Aug. 2018.

[29] C. Le Coq and H. Orzen, "Price caps and fluctuating demands in electricity markets: Experimental evidence of competitive bidding," in *Proceedings of 2012 9th International Conference on the European Energy Market*, Florence, Italy, May 2012, pp. 1-4.

[30] J. Yao, S. S. Oren, and I. Adler, "Two-settlement electricity markets with price caps and Cournot generation firms," *European Journal of Operational Research*, vol. 181, no. 3, pp. 1279-1296, Sept. 2007.

[31] S. Cowan, "Price-cap regulation," *Swedish Economic Policy Review*, vol. 9, no.2, pp. 167-188, Jan. 2022.

[32] Z. Yan and Y. Xu, "A multi-agent deep reinforcement learning method for cooperative load frequency control of a multi-area power system," *IEEE Transactions on Power Systems*, vol. 35, no. 6, pp. 4599-4608, Nov. 2020.

[33] R. Chen, D. Ke, Y. Sun *et al*., "Hierarchical frequency-dependent chance constrained unit commitment for bulk AC/DC hybrid power systems with wind power generation," *Journal of Modern Power Systems and Clean Energy*, vol. 11, no. 4, pp. 1053-1064, Jul. 2023.

[34] F. Zhao, E. Litvinov, and T. Zheng, "A marginal equivalent decomposition method and its application to multi-area optimal power flow problems," *IEEE Transactions on Power Systems*, vol. 29, no. 1, pp. 53-61, Jan. 2014.

[35] S. Huang, Y. Sun, and Q. Wu, "Stochastic economic dispatch with wind using versatile probability distribution and L-BFGS-B based dual decomposition," *IEEE Transactions on Power Systems*, vol. 33, no. 6, pp. 6254-6263, Nov. 2018.

[36] A. Tosatto, T. Weckesser, and S. Chatzivasileiadis, "Market integration of HVDC lines: internalizing HVDC losses in market clearing," *IEEE Transactions on Power Systems*, vol. 35, no. 1, pp. 451-461, Jan. 2020.

[37] Q. Xu, N. Zhang, C. Kang *et al*., "A game theoretical pricing mechanism for multi-area spinning reserve trading considering wind power uncertainty," *IEEE Transactions on Power Systems*, vol. 31, no. 2, pp. 1084-1095, Mar. 2016.

[38] J. Wang, H. Zhong, Z. Yang *et al.*, "Incentive mechanism for clearing energy and reserve markets in multi-area power systems," *IEEE Transactions on Sustainable Energy*, vol. 11, no. 4, pp. 2470-2482, Oct. 2020.

[39] J. Ma, F. B. B. Rolim, A. Elkasrawy *et al.*, "A zonal capacity market model with energy storage for transmission and distribution," *IEEE Open Access Journal of Power and Energy*, vol. 9, pp. 398-408, Aug. 2022.

[40] C. Lin, H. Liang, A. Pang *et al.*, "Data-driven surrogate-assisted method for high-dimensional multi-area combined economic/emission dispatch," *Journal of Modern Power Systems and Clean Energy*, vol. 12, no. 1, pp. 52-64, Jan. 2024.

[41] J. Zhu, X. Mo, Y. Xia *et al.*, "Fully-decentralized optimal power flow of multi-area power systems based on parallel dual dynamic programming," *IEEE Transactions on Power Systems*, vol. 37, no. 2, pp. 927-941, Mar. 2022.

[42] L. L. Kiesling, *Deregulation, Innovation and Market Liberalization: Electricity Regulation in a Continually Evolving Environment*. London: Routledge, 2008.

[43] R. Rahmaniani, T. G. Crainic, M. Gendreau *et al.*, "The Benders decomposition algorithm: a literature review," *European Journal of Operational Research*, vol. 259, no. 3, pp. 801-817, Jun. 2017.

[44] B. Zeng and L. Zhao, "Solving two-stage robust optimization problems using a column-and-constraint generation method," *Operations Research Letters*, vol. 41, no. 5, pp. 457-461, Sept. 2013.

[45] T. L. Magnanti and R. T. Wong, "Accelerating Benders decomposition: algorithmic enhancement and model selection criteria," *Operations Research*, vol. 29, no. 3, pp. 464-484, Jun. 1981.

[46] N. B. Asl and S. A. MirHassani, "Accelerating Benders decomposition: multiple cuts via multiple solutions," *Journal of Combinatorial Optimization*, vol. 37, no. 3, pp. 806-826, Apr. 2019.

[47] P. Wang, Q. Wu, S. Huang *et al.*, "ADMM-based distributed active and reactive power control for regional AC power grid with wind farms," *Journal of Modern Power Systems and Clean Energy*, vol. 10, no. 3, pp. 588-596, May 2022.

[48] J. Ostrowski, M. F. Anjos, and A. Vannelli, "Tight mixed integer linear programming formulations for the unit commitment problem," *IEEE Transactions on Power Systems*, vol. 27, no. 1, pp. 39-46, Feb. 2012.

[49] G. Morales-España, J. M. Latorre, and A. Ramos, "Tight and compact MILP formulation for the thermal unit commitment problem," *IEEE Transactions on Power Systems*, vol. 28, no. 4, pp. 4897-4908, Nov. 2013.

[50] F. Li and R. Bo, "DCOPF-based LMP simulation: algorithm, comparison with ACOPF, and sensitivity," *IEEE Transactions on Power Systems*, vol. 22, no. 4, pp. 1475-1485, Nov. 2007.

[51] F. Li and Q. Zhang. (2024, May). ENLITEN-Grid-Econ-Data. [Online]. Available: https://github.com/enliten/ENLITEN-Grid-Econ-Data

[52] N. Parsly, J. Wang, N. West *et al.*, "DiME and AGVis: a distributed messaging environment and geographical visualizer for large-scale power system simulation," in *Proceedings of 2023 North American Power Symposium (NAPS)*, Asheville, USA, Oct. 2023, pp. 1-5.

[53] F. Li, K. Tomsovic, and H. Cui, "A large-scale testbed as a virtual power grid: for closed-loop controls in research and testing," *IEEE Power and Energy Magazine*, vol. 18, no. 2, pp. 60-68, Mar.-Apr. 2020.

Sufan Jiang received the B.S.E.E., M.S.E.E., and Ph.D. degrees from Southeast University, Nanjing, China, in 2014, 2017, and 2022, respectively. Currently, he is a Research Scientist at the University of Tennessee, Knoxville (UTK), USA. His research interests include resilience, flexibility, and energy policy in power system.

Fangxing (Fran) Li received the B.S.E.E. and M.S.E.E. degrees from Southeast University, Nanjing, China, in 1994 and 1997, respectively, and the Ph.D. degree from Virginia Tech, Blacksburg, USA, in 2001. Currently, he is the James W. McConnell Professor in electrical engineering at the University of Tennessee, Knoxville (UTK), USA. He is also a Founding Member of CURENT, an NSF/DOE Engineering Research Center headquartered at UTK, and serves as the UTK Campus Director of CURENT. His current research interests include renewable energy integration, demand response, distributed generation and microgrid, electricity market, and power system computing.

Xiaofei Wang received the B.S.E.E. degree from North China Electric Power University, Beijing, China, the M.S.E.E. degree from Wuhan University, Wuhan, China, and the Ph.D. degree from the University of Tennessee, Knoxville, USA, in 2014, 2017, and 2023, respectively. His research interests include distribution-level electricity market, power system optimization, and demand response.

Chenchen Li received the B.S.E.E. and M.S.E.E. degrees from North China Electric Power University, Beijing, China, in 2019 and 2022, respectively. She is currently working toward the Ph.D. degree in electrical engineering at The University of Tennessee, Knoxville, USA. Her research interests include distribution system optimization, distribution system planning, and energy equity in power system.